Volume 8 | Number 12 | 21 June 2021

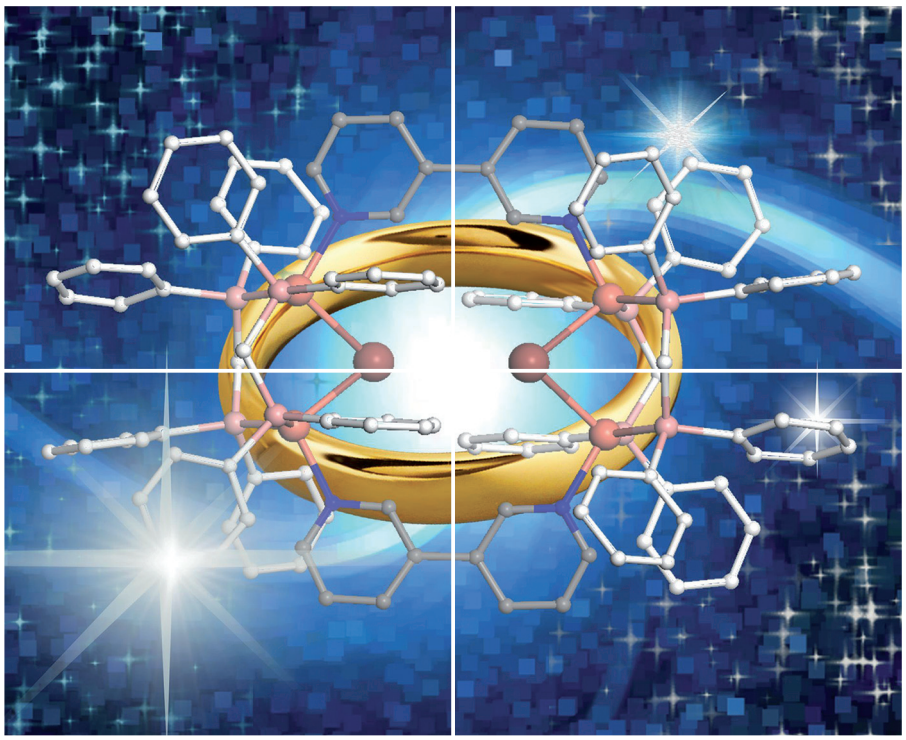

ORGANIC CHEMISTRY

FRONTIERS

CCS 中国化学会 CHINESE CHEMICAL SOCIETY

SIOC 1950

ROYAL SOCIETY OF CHEMISTRY

rsc.li/frontiers-organic

ORGANIC CHEMISTRY FRONTIERS

RESEARCH ARTICLE

View Article Online
View Journal | View Issue

Cite this: *Org. Chem. Front.*, 2021, **8**, 2893

Self-assembled luminescent Cu(I) tetranuclear metallacycles based on 3,3′-bipyridine ligands†

Florent Moutier, Jana Schiller, Guillaume Calvez * and Christophe Lescop *

Received 7th April 2021,
Accepted 11th May 2021

DOI: 10.1039/d1qo00538c

rsc.li/frontiers-organic

3,3′-Bipyridine ligand **B** was reacted with pre-assembled $[Cu_2(\mu_2\text{-dppm})_2]$ Cu(I) bimetallic flexible precursor **A** according to coordination-driven supramolecular chemistry synthetic principles. Outcomes obtained revealed the necessity to formally introduce bridging halide X ions (X = Cl, Br or I) in order to conduct selectively and successfully coordination-driven supramolecular syntheses. Therefore, $[Cu_2(\mu_2\text{-dppm})_2(\mu_2\text{-X})]$ bimetallic connecting nodes presenting a potential coordination angle of *ca.* 120° are generated, which lead upon reaction with connecting ligand **B** to the selective formation of new tetranuclear metallacycles $\mathbf{C_X}$. These derivatives are luminescent in the solid-state at room temperature with high emission quantum yields and a study of the temperature dependence of their photophysical properties was conducted, suggesting a ligand **B** centered triplet origin for their luminescence.

Introduction

A fruitful and appealing alternative to classic synthetic methodologies for constructing complex discrete molecular scaffolds consists of the application of supramolecular self-assembly procedures.[1] In these approaches, the spontaneous recognition of rationally designed individual building blocks occurs, affording selectively well-defined discrete supramolecular architectures. These self-assembly processes are promoted by non-covalent kinetically labile bond formations, which take place along self-sorting and self-correction events until the individual building blocks gather into the final thermodynamically stable target product. Considering in this context the use of the metal–ligand coordination interaction, a plethora of multimetallic supramolecular assemblies have blossomed in the last decade,[2,3] in particular according to coordination driven supramolecular (CDS) chemistry synthetic principles.[3] CDS processes rely on the use of pre-organized coordination complexes having predefined geometries (being in most cases hardly accessible from a single metal center coordination sphere) and vacant coordination positions.[3] These pre-organized precursors, obtained from the reaction of metal ions with specific assembling ligands, are associated with connecting polytopic ligands allowing the formation of targeted multimetallic derivatives whose sizes and geometries are controlled by the symmetry of the linking sites of the individual building blocks. According to this synthetic approach, a variety of attractive multifunctional molecular devices or metallacages bearing remarkable ability for the selective encapsulation of certain guest species and/or original reactivity within their internal confined spaces could thus be prepared.[3] Within the intricate CDS polymetallic assemblies reported, metallo-macrocycles are omnipresent. They constitute either the targeted scaffolds or serve as sub-units for the construction of more elaborated molecular architectures. So far, CDS systems based mostly on the Pt(II) and Pd(II) metal centers have been flourishing.[2n–u,3a–d,4] Indeed, these ions combine strong preferences for a rigid square planar coordination sphere and highly directional thermodynamically stable but kinetically labile metal–ligand interactions with a large range of ligating coordination groups, which are key factors to ensure the success of CDS synthetic processes. Yet, in recent years, alternatives to these leading trends have appeared allowing the introduction of a larger variety of metal centers and ligating groups.[5]

Thus, we have recently initiated the introduction of pre-assembled Cu(I) precursors such as the $[Cu_2(\mu_2\text{-dppm})_2]^{2+}$ bimetallic fragment **A** (Scheme 1a, dppm = bis(diphenylphosphino)methane) in self-assembly procedures related to CDS syntheses.[6] In these cases, the typical labile, flexible and low-directional coordination sphere of this ion, initially regarded *a priori* as strongly restrictive in conventional CDS chemistry, turned out to be very valuable to conduct the selective preparation of original CDS assemblies based on the Cu(I) ion. In addition, the obtained polymetallic derivatives present a variety of luminescence properties[7] due to the versatile photophysical processes lying in Cu(I)-based derivatives (such as Thermally Activated Delayed Fluorescence (TADF)),[7a,c] drawing

Univ Rennes, INSA Rennes, CNRS, ISCR (Institut des Sciences Chimiques de Rennes) – UMR 6226, F-35000 Rennes, France. E-mail: christophe.lescop@insa-rennes.fr

† Electronic supplementary information (ESI) available. CCDC 2074606–2074608. For ESI and crystallographic data in CIF or other electronic format see DOI: 10.1039/d1qo00538c

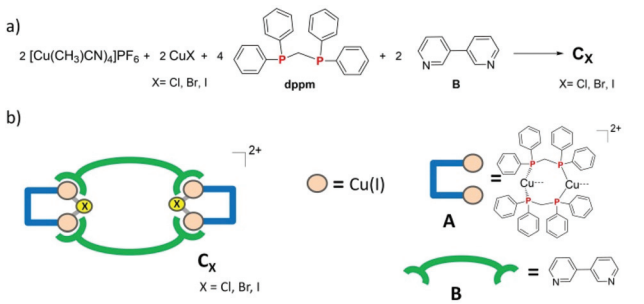

Scheme 1 a) Synthesis of derivatives $\mathbf{C_x}$; (b) schematic representation of derivatives $\mathbf{C_x}$.

new perspectives in the ready design of innovative and inexpensive luminescent supramolecular compounds. Very importantly, these previous studies highlighted a win–win situation, promoting the introduction of Cu(I) metal centers in attractive luminescent CDS assemblies. Indeed, on the one hand, the integration of the Cu(I) ions within CDS intricate scaffolds bearing multiple chelates and metallacycle sub-units endows this Cu(I)-based species with significant thermodynamic stability. Therefore, selective self-assembly processes toward a single product can be directed in solution. This is a marked contrast compared to the multiple equilibria typical of the fluxionality of Cu(I) metal centres' coordination spheres that can govern the conventional solution coordination chemistry of the Cu(I) ion and frequently result in unpredictable mixtures of hetero- and homoleptic structures.[8] Moreover, this has allowed establishing that due to a suitable molecular design of pre-assembled Cu(I) polymetallic building blocks, it is possible to proceed to the rationalization of the adaptative behaviors exhibited by the intrinsically conformationally flexible polymetallic Cu(I) precursors used.[6a,c] On the other hand, in these CDS assemblies, the Cu(I) metal centers are embedded within polycyclic supramolecular scaffolds having constrained geometries. These metal centers are thus subject to the significantly reduced possibility of structural re-organization of their coordination sphere in the excited states. Therefore, the non-radiative deactivation pathways associated with such re-organization are greatly minimized within Cu(I)-based CDS assemblies which promotes the emergence of enhanced photophysical properties in such self-assembled derivatives.

Taking these observations into consideration, we have been motivated to explore further the use of CDS chemistry for the selective preparation of new luminescent Cu(I) metallacycles. Herein, we describe the one-step preparation of three new tetranuclear dicationic discrete metallacycles $\mathbf{C_X}$ (X = Cl, Br, I). Their synthesis, characterization, X-ray single crystal molecular structure and solid-state luminescence properties are reported.

Results and discussion

While previous preparation of Cu(I)-based CDS luminescent assemblies mostly focused on the use of cyano-based inorganic linkers[6] and nitrile-terminated organic ditopic ligands,[9] we have been interested to extend these investigations to the reaction of the pre-organized $[Cu_2(\mu_2\text{-dppm})_2]^{2+}$ bimetallic fragment **A** with pyridyl-terminated organic ligands. Indeed, such electron-rich nitrogen-donor polytopic linkers predominate in CDS syntheses due to the strong affinity of these moieties toward a large variety of metal ions and due to the high directionality of the coordination bonds formed. In this study, we have focussed more particularly on the use of the ditopic 3,3′-bipyridine ligand **B** since it was demonstrated that bis-monodentate ligands bearing the 3-pyridyl moiety as a coordinating group present a strong tendency to form discrete polycyclic CDS-assemblies.[2d,u,v,3e,4b] Moreover, luminescent Cu(I) coordination polymers have been previously reported bearing **B** as the connecting ligand between the metal centers,[10] demonstrating the appealing photophysical properties that can arise from the association of Cu(I) metal centers with **B**. In the course of this study, we have observed that it is mandatory to introduce an additional μ_2-bridging halide anion on the Cu(I) bimetallic unit of the pre-assembled $[Cu_2(\mu_2\text{-dppm})_2]^{2+}$ precursor, in order to prepare selectively new Cu(I) discrete polymetallic derivatives. Indeed, when one equivalent of the *in situ* formed $[Cu_2(\mu_2\text{-dppm})_2]^{2+}$ unit was reacted in CH_2Cl_2 under air at room temperature (RT) with one equivalent of ligand **B** a colourless clear solution was obtained. The slow diffusion of pentane vapors in this solution afforded after a few days a mixture of different colourless polycrystalline species having a significantly distinct eye-perceived luminescence color under UV-Vis light excitation (λ_{ex} = 365 nm), ranging from blue-green to yellow. Unfortunately, the quality of these crystallites and their very low stability once removed from the mother solution did not allow us to determine their X-ray crystal structures. It was also not possible to purify these species *via* manual separation since the crystals collapsed in polycrystalline powder very quickly once removed from the mother solution. Yet, after a few weeks, we observed that a small amount of well-shaped new colorless crystals of the species $\mathbf{C_{Cl}}$ appeared in the crystallisation experiments. These crystals display at RT in the solid state an eye-perceived blue-cyan intense luminescence upon UV-Vis light excitation (λ_{ex} = 365 nm) and could be successfully collected in order to establish the solid-state molecular structure of $\mathbf{C_{Cl}}$, thanks to a single crystal X-ray diffraction study experiment performed at low temperature. It revealed that this compound crystallizes in the triclinic space group $P\bar{1}$ (Table 1) with an asymmetric unit containing half of the discrete supramolecular assembly $\mathbf{C_{Cl}}$, one hexafluorophosphate counter-anion and five disordered CH_2Cl_2 solvent molecules. The derivative $\mathbf{C_{Cl}}$ is a centrosymmetric dicationic tetrametallic metallacycle (Scheme 1b, Fig. 1) resulting from the connection of two $[Cu_2(\mu_2\text{-dppm}_2)(\mu_2\text{-Cl})]^+$ dimeric units by two **B** ligands acting as ditopic linkers. The metal centers present similar $P_2Cl_1N_1$ distorted tetrahedral coordination spheres (Table 2) and, compared to the other Cu(I) polymetallic assemblies based on this bimetallic unit, the overall metric data at the $[Cu_2(\mu_2\text{-dppm})_2]$ sub-unit are classical.[6,9] Yet, the intermetallic distance is quite

Table 1 Crystal data and structural refinement of derivatives C_{Cl}, C_{Br} and C_I after squeeze treatment (values in italics are related to the relevant data before the squeeze treatment)

	C_{Cl}	C_{Br}	C_I
Molecular formula	$C_{120}H_{104}Cl_2Cu_4F_{12}N_4P_{10}$ *($C_{130}H_{112}Cl_{22}Cu_4F_{12}N_4P_{10}$)*	$C_{120}H_{104}Br_2Cu_4F_{12}N_4P_{10}$ *($C_{130}H_{112}Br_2Cl_{20}Cu_4F_{12}N_4P_{10}$)*	$C_{120}H_{104}I_2Cu_4N_4P_8$ *($C_{132}H_{98}I_2Cl_{24}Cu_4F_{12}N_4P_{10}$)*
CCDC	2074606	2074608	2074607
Molecular weight	2464.83 *(3302.00)*	2553.75 *(3390.92)*	2357.79 *(3636.60)*
a (Å)	14.113(2)	14.182(3)	14.308(2)
b (Å)	14.181(2)	14.237(3)	14.297(2)
c (Å)	18.602(2)	18.585(3)	18.459(2)
α (°)	87.110(4)	87.431(6)	68.40156
β (°)	69.039(4)	69.448(5)	87.648(5)
γ (°)	84.128(4)	84.493(6)	85.23156
V (Å^3)	3458.0(8)	3497.2(12)	3498.7(3)
Z	1	1	1
D_c (g cm^{-3})	1.184 *(1.586)*	1.213 *(1.610)*	1.119 *(1.726)*
Crystal system	Triclinic	Triclinic	Triclinic
Space group	$P\bar{1}$	$P\bar{1}$	$P\bar{1}$
Temperature (K)	150(2)	150(2)	150(2)
Wavelength Mo-Kα (Å)	0.71069	0.71069	0.71069
Crystal size (mm)	0.35 × 0.28 × 0.11	0.45 × 0.11 × 0.09	0.16 × 0.11 × 0.07
μ (mm^{-1})	0.819 *(1.215)*	1.343 *(1.734)*	1.171 *(1.682)*
F(000)	1260 *(1668)*	1296 *(1704)*	1194 *(1806)*
θ limit (°)	2.02–27.57	2.19–27.63	2.17–27.55
Index ranges *hkl*	$-18 < h < 18$ $-17 < k < 18$ $-24 < l < 24$	$-18 < h < 18$ $-18 < k < 15$ $-24 < l < 24$	$-18 < h < 18$ $-17 < k < 18$ $-23 < l < 23$
Reflections collected	*70 583*	55 169	56 861
Independent reflections	*15 920*	15 866	15 846
Reflections [$I > 2\sigma(I)$]	12 697 *(12 710)*	12 432 *(12 827)*	10 729 *(10 872)*
Data/restraints/parameters	15 920/0/719 *(15 920/0/854)*	15 866/0/709 *(15 866/0/854)*	15 846/0/622 *(15 846/0/875)*
Goodness-of-fit on F^2	1.088 *(1.058)*	1.088 *(1.042)*	1.105 *(0.988)*
Final R indices [$I > 2\sigma(I)$]	R_1 = 0.0680 *(0.0891)* wR_2 = 0.1995 *(0.2353)*	R_1 = 0.0852 *(0.1127)* wR_2 = 0.2290 *(0.2853)*	R_1 = 0.0857 *(0.1143)* wR_2 = 0.2219 *(0.2866)*
R indices (all data)	R_1 = 0.0802 *(0.1082)* wR_2 = 0.2110 *(0.2568)*	R_1 = 0.1009 *(0.1329)* wR_2 = 0.2418 *(0.3035)*	R_1 = 0.1188 *(0.1607)* wR_2 = 0.2413 *(0.3248)*
Largest diff peak and hole (e Å^{-3})	1.483 and −1.383 *(2.209 and −1.730)*	2.452 and −1.635 *(4.816 and −1.559)*	2.247 and −1.797 *(3.434 and −1.857)*

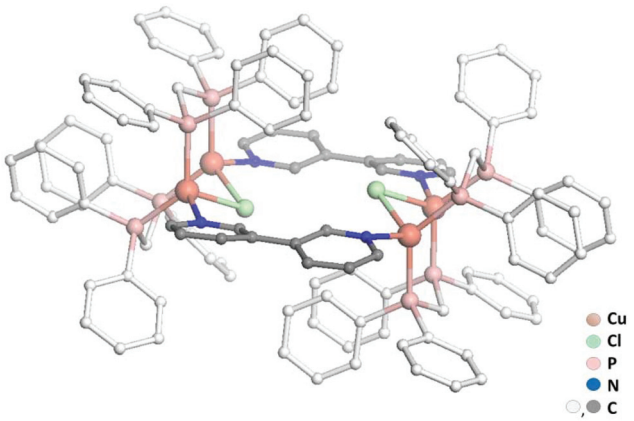

Fig. 1 (a) Views of the molecular X-ray structures of dicationic metallacycle C_{Cl} (counteranions, H atoms and solvent molecules have been omitted for clarity).

large (d(Cu–Cu) = 3.179(7) Å, above the limit usually proposed for cuprophilic interactions)[11] as a result of the presence of a μ_2-symetrically bridging chloro ligand (d(Cu–Cl) = 2.4034(12) and 2.4048(11) Å). Within assembly $\mathbf{C_{Cl}}$, the two μ_2-chloro ligands (separated by *ca.* 4.55 Å) are located toward the center of the metallacycle and are orientated slightly outward of the mean plane defined by the four Cu(I) ions (deviation to the mean plane: 0.753 Å). The coordination of ligands **B** on the two metal centers of the bimetallic units is also highly symmetrical with similar (Cu–Cu–N) angles (150.21 and 150.34°) and (Cu–N) bond lengths (both being 2.121(3) Å). The torsion angle between the two 6-membered rings of coordinated ligands **B** is 17.2° (Fig. 2c), which is significantly smaller than the torsion angle (43.6°) found in the previously reported Cu(I) 1D-CP based on ligand **B**, in which in addition shorter (Cu–N) bond lengths have been observed (d(Cu–N) = 2.034(3) Å).[10] This highlights the steric constraints applied on the backbone of coordinated ligands **B** within the metallacyclic scaffold of $\mathbf{C_{Cl}}$.

The origin of the bridging μ_2-chloro ligand probably arises from slow chloride abstraction from CH_2Cl_2 solvent molecules under the crystallization conditions applied. Similar examples that involve chloride abstraction have also been observed for the preparation of other multi-nuclear copper complexes.[12] Yet, considering the very slow crystallisation process of the metallacycle $\mathbf{C_{Cl}}$, it is very likely that equilibria

Table 2 Selected intermetallic distances [Å] and angles [°] in derivatives C_{Cl}, C_{Br} and C_I

	C_{Cl}	C_{Br}	C_I
Cu–Cu	3.180(4)	3.261(5)	3.362(5)
Cu–N	2.121(3) and 2.121(3)	2.109(4) and 2.121(5)	2.119(6) and 2.124(5)
Cu–X	2.4034(12) and 2.4048 (11)	2.5218(11) and 2.5211(10)	2.6646(11) and 2.6636(12)
Cu–P	2.2687(10), 2.2569(10), 2.2604(11) and 2.2527(11)	2.2682(15), 2.2567(14), 2.2595(16) and 2.2546(16)	2.2474(17), 2.2576(16), 2.2549(19) and 2.2539(19)
Cu–Cu–N	150.25(3), 150.37(4)	150.76(5), 150.27(6)	151.51(5), 151.15(5)
Cu–X–Cu	82.80(3)	80.58(2)	78.24(3)

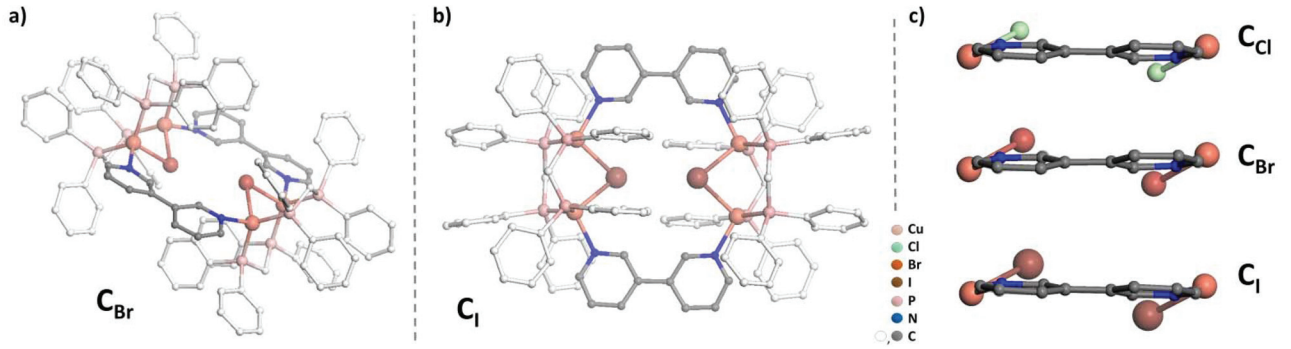

Fig. 2 Views of the molecular X-ray structures (counteranions, H atoms and solvent molecules have been omitted for clarity) of the dicationic derivatives (a) C_{Br} and (b) C_I; (c) simplified 'lateral' views of the X-ray structures of metallacycles C_{Cl}, C_{Br} and C_I.

occur in the crystallisation tubes in which reactive secondary species are able to trap chloride atoms arising from CH_2Cl_2 solvent degradation. Indeed, after two additional months, the amount of crystals of C_{Cl} did not increase significantly, precluding further characterisation of this metallacycle at that stage.

Yet, this result suggests that the introduction of a μ_2-bridging chloro ligand on the $[Cu_2(\mu_2\text{-dppm})_2]^{2+}$ building unit could favour the preparation of stable metallacyclic species based on ligand **B**, by forcing this conformationally flexible $[Cu_2(\mu_2\text{-dppm})_2]^{2+}$ fragment to adopt a suitable geometry promoting selective self-association processes.

In order to confirm this assumption, a CH_2Cl_2 solution of one equivalent of $[Cu((CH_3)CN)_4]PF_6$, one equivalent of CuCl and two equivalents of the dppm ligand was prepared (Scheme 1a) and left upon stirring at room temperature (RT) under air for one hour, affording a colorless solution. To this solution one equivalent of ligand **B** dissolved in CH_2Cl_2 was added, leading to a slightly yellowish colored clear solution that was left upon stirring at RT overnight. The crude solution was then left to crystallize under air at RT upon pentane vapor diffusions. After one week a homogeneous batch of well-shaped single crystals was obtained, which were identified by a single crystal X-ray diffraction study as crystals of metallacycle C_{Cl}. After filtration, the sample was dried affording a homogeneous sample of a block-shaped colorless polycrystalline solid of C_{cl} with a yield of 66%.

Thus, the presence of chloride anions in the synthesis conducted induces complete alteration of the self-assembly processes occurring as the pre-assembled $[Cu_2(\mu_2\text{-dppm})_2]^{2+}$ precursor is reacted with ligand **B**. Indeed, instead of a mixture of unidentified species obtained in the first step, followed by a very slow and low-efficient conversion to derivative C_{Cl}, this metallacycle can be directly and selectively obtained in good yield if CuCl is introduced in the reaction. Along this synthetic procedure, formally, a $[Cu_2(\mu_2\text{-dppm})_2(\mu_2\text{-Cl})]^+$ moiety can be considered as being formed as a pre-assembled building unit. Such an *in situ* formed precursor presents very likely a significantly restricted degree of conformation freedom compared to the $[Cu_2(\mu_2\text{-dppm})_2]^{2+}$ fragment since the μ_2-bridging chloro ligand locks the geometry of the bimetallic unit. This results in the formation of a bimetallic rigid $[Cu_2(\mu_2\text{-dppm})_2(\mu_2\text{-Cl})]^+$ connecting node bearing potentially two available coordination positions (one on each metal center) with a coordination angle of *ca.* 120°. In such a situation, selective CDS assembling processes take place along which ligand **B** is forced to adopt a N,N cisoid orientation of its two 3-pyridyl fragments resulting in the ready and selective formation of the metallacycle backbone of C_{Cl}.

Importantly, this approach affording new Cu(I) CDS metallacyles is not only restricted to the introduction of a μ_2-bridging chloro ligand on the Cu(I) bimetallic building blocks. Using CuBr or CuI instead of CuCl (Scheme 1a), new metallacycles C_{Br} and C_I could also be obtained selectively according

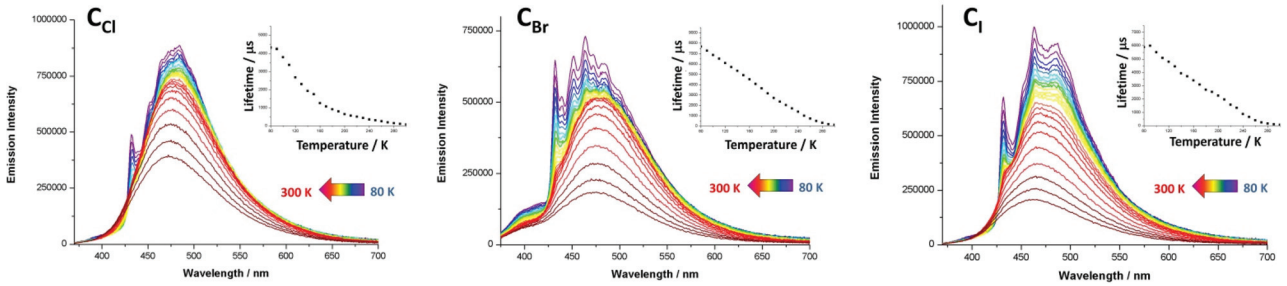

Fig. 3 Temperature dependence (80 K to 300 K) of the solid-state emission spectra of metallacycles C_{Cl}, C_{Br} and C_I upon excitation at 325 nm.‡ Inset: plot of their emission decay lifetime against temperature (80 K to 300 K).

to a similar synthetic procedure. X-ray diffraction studies revealed that the crystals of these compounds are isostructural with those of $\mathbf{C_{Cl}}$ (Table 1), gathering two $[Cu_2(\mu_2\text{-dppm})_2(\mu_2\text{-X}]$ (X = Br or I) bimetallic building blocks in the tetrametallic metallacycle *via* their coordination with two **B** ligands (Fig. 2a and b). Within these dicationic assemblies, the intermetallic distance increases ($\mathbf{C_{Br}}$: 3.261(8) Å; $\mathbf{C_I}$: 3.362(7) Å) with the atomic radius of the bridging halide atom but the μ_2-symetrically bridging coordination mode is preserved along the series ($\mathbf{C_{Br}}$: *d*(Cu–Br) = 2.5211(10) and 2.5218(11) Å; $\mathbf{C_I}$: *d*(Cu–I) = 2.6636(12) and 2.6646(11) Å, Table 2). Inside these metallacycles, the deviations of the μ_2-bridging halide ions from the mean plane defined by the four Cu(I) ions ($\mathbf{C_{Br}}$: 0.812 Å; $\mathbf{C_I}$: 0.884 Å) are similar to the value found in derivative $\mathbf{C_{Cl}}$. Regarding the coordination displayed by connecting ligands **B**, moderate differences are observed along the series of the three derivatives $\mathbf{C_{cl}}$, $\mathbf{C_{Br}}$ and $\mathbf{C_I}$, in which the (Cu–Cu–N) angles are also symmetrical (150.27° and 150.76° in $\mathbf{C_{Br}}$; 151.15° and 151.51° in $\mathbf{C_I}$). The (Cu–N) bond lengths are 2.109(4) Å and 2.121(5) Å in $\mathbf{C_{Br}}$ and 2.119(6) Å and 2.124(5) Å in $\mathbf{C_I}$ and therefore do not significantly differ from the values observed in $\mathbf{C_{Cl}}$ (Table 2). Finally, the torsion angle between the two rings of the coordinated ligands **B** is 15.9° in $\mathbf{C_{Br}}$ and 9.8° in $\mathbf{C_I}$ (Fig. 2c), confirming thus that ligands **B** within these assemblies are forced upon coordination to present a remarkable planarity whose extent is enhanced as the μ_2-symetrically bridging ligand changes from chloride to bromide and to iodide. Therefore, in the molecular structure of a series of tetrametallic metallacycles $\mathbf{C_x}$ (X = Cl, Br, I), the variation of the nature of the μ_2-bridging halide mostly affects the metric data at the Cu(I) dimer and the conformation presented by ligands **B**, but the gross molecular structures are similar. Interestingly, a related Cu(I) complex of tetramesityl substituted ferrocene bisphosphine $[Fe(CpPMes_2)_2{}^*(CuBr)_2]_2$, which presents a comparable metallacyclic structure in which Cu(I) dimers are bridged by μ_2-bromide atoms, was recently described by Pietschnig *et al.*[13] In this derivative, the intermetallic distance in the Cu(I) dimer (*d*(Cu–Cu) = 2.93 Å) is shorter than that in $\mathbf{C_{Br}}$ and the deviations from the mean plane defined by the four Cu(I) ions of 1.135 Å are significantly larger than those observed in $\mathbf{C_{Br}}$ suggesting overall larger steric constrains within this metallacycle core.

The crystals of $\mathbf{C_{Cl}}$, $\mathbf{C_{Br}}$ and $\mathbf{C_I}$ are colorless under visible light and display under UV irradiation (λ_{ex} = 365 nm) eye-perceived light blue-cyan solid-state RT luminescence. The solid-state RT UV-visible absorption spectra of derivatives $\mathbf{C_{Cl}}$, $\mathbf{C_{Br}}$ and $\mathbf{C_I}$ (Fig. S10–12†) exhibit a strong and broad absorption band in the near UV region centered at *ca.* 300 nm, typical of π–π^* transition centered on the aromatic rings of dppm and ligands **B**. The excitation spectra (Fig. S4–S6†) of these compounds reveal two maxima at *ca.* 325 nm and *ca.* 370 nm. In their emission spectra, derivatives $\mathbf{C_{Cl}}$, $\mathbf{C_{Br}}$ and $\mathbf{C_I}$ display at 300 K a broad featureless band centered at λ_{max} = 475, 476 and 464 nm respectively (Fig. 3 and Table 3).‡ In the solid state, these compounds present RT lifetimes of the excited state of 74 µs, 119 µs and 70 µs and their RT emission quantum yields (EQYs) reach 80%, 60% and 54% for $\mathbf{C_{Cl}}$, $\mathbf{C_{Br}}$ and $\mathbf{C_I}$ respectively.§ Such solid-state RT EQY values are remarkably high for derivatives bearing RT lifetimes whose values of several tenths of microseconds indicate a triplet origin for the luminescence observed. Moreover, the RT EQY value progression is reversed compared to the increase of the atomic number of the μ_2-bridging halide ligand. This is quite unusual in luminescent Cu(I)-halide derivatives in which the increment of the spin–orbit coupling associated with heavier halides usually promotes efficient radiative relaxation processes *via* external heavy-atom effects. To gain more insights into the emission properties of derivatives $\mathbf{C_{Cl}}$, $\mathbf{C_{Br}}$ and $\mathbf{C_I}$, temperature dependent photophysical characterization was conducted upon cooling the temperature from 300 K to 80 K. In the emission spectra of $\mathbf{C_{Cl}}$ under excitation at 325 nm,‡ a gradual and very moderate red-shift (Fig. 3) of the large band observed upon cooling at 300 K (λ_{max} = 475 nm) is observed with a net increase of the signal intensity. This intensity enhancement is accompanied at the lowest temperature by progressive structuration of the emission band yielding at 80 K a large signal bearing an apparent vibronic sub-structure with two maxima centered at 432 and 484 nm (for which is observed the highest intensity signal) and three shoulders at 452, 465 and 502 nm (Table 3).

‡These temperature dependant behaviour do not depend on the excitation energy and similar results were obtained with λ_{ex} = 375 nm.
§These emission decay times are mono-exponential.

Table 3 Photophysical data (λ_{ex} = 325 nm) for derivatives C_{Cl}, C_{Br} and C_I at 298 K and 80 K in the solid state

	λ_{em} [a] (nm)	Φ_{em}	τ_{obs} [a] (μs)	k_r [b] (s^{-1})	k_{nr} [c] (s^{-1})
$\mathbf{C_{Cl}}$	475 (432, 452,[s] 465,[s] 484, 502[s])	80	74 (4315)	1.1×10^4	2.7×10^3
$\mathbf{C_{Br}}$	476 (432, 452, 464, 484,[s] 500[s])	60	119 (7660)	5.0×10^3	3.4×10^3
$\mathbf{C_I}$	464 (432, 452,[s] 462, 486, 50[s])	54	70 (5881)	7.7×10^3	6.6×10^5

[a] Data recorded at 80 K are given in parentheses. [b] $k_r = \Phi_{em}/\tau_{obs}$. [c] $k_{nr} = (1 - \Phi_{em})/\tau_{obs}$; [s]: shoulder.

Regarding the thermal variation of the lifetimes of the excited state of $\mathbf{C_{Cl}}$, a continuous and significant increase of the decay time is observed upon cooling, reaching 4.3 ms at 80 K (Fig. 3, Table 3).§ Comparable temperature dependent profiles are observed for the emission spectra and the lifetimes of the excited state of $\mathbf{C_{Br}}$ and $\mathbf{C_I}$ (Fig. 3 and Table 3). In comparison, the low temperature emission spectrum of free ligand **B** (Fig. S16†) is characterized by a large unstructured band centred at 455 nm (λ_{ex} = 320 nm) associated with a considerably shorter decay time of the excited state (4.5 ns) at 80 K, typical of purely organic fluorescence. Note that in the temperature dependent emission spectra of derivative $\mathbf{C_{Br}}$ (Fig. 3) a weak and large additional band appears between 375 and 425 nm associated with a decay time of the excited state of 3.5 ns that can likely be assigned to the residual ligand centred luminescence.

The values of the recorded emission lifetimes clearly indicate a triplet origin of the luminescence arising from these Cu(I) metallacycles and, together with the general thermal variation of the profiles of the emission spectra, preclude to suggest a TADF process to explain the overall temperature-dependent data collected for the photophysical properties of these three metallacycles, in spite of the high RT EQY measured.

Regarding specifically the RT photophysical behaviors for this series of metallacycles, the k_r radiative rate constant values are in agreement with ^{3}MLCT phosphorescence in which the high temperature large emission bands can be assigned to radiative processes involving likely electronic densities located on 3,3′-bipyridine ligands **B**. Yet, the large enhancement of the decay times of the excited states as the temperature decreases, together with the vibronic structuration that appears in the low temperature emission band, suggests at low temperature $^3\pi$–π^* ^{3}ILCT phosphorescence centered on the connecting ligands **B**. Such a vibronic structuration is indeed not observed in the thermal variation of related TADF luminescent polymetallic supramolecular assemblies based on the $[Cu_2(\mu_2\text{-dppm})_2]$ moiety and cyano-based connecting inorganic ligands,[6b–d] in which radiative processes mostly rely on transitions from the highest occupied molecular orbitals (HOMOs), being metal-cyano antibonding, to the lowest unoccupied molecular orbital (LUMO) having MLCT character involving the four metal centres of the metallacycle and the dppm ligands. Conversely, in a 1D-coordination polymer based on related $[Cu_2(\mu_2\text{-dppm})_2(\mu_2\text{-OH}_2]^{2+}$ dicationic fragments connected by 1,4-dicyanobenzene connecting ditopic ligands,[9d] similar progressive structuration of the emission band is observed upon cooling the temperature. In the case of this 1D-coordination polymer, the low temperature photophysical properties were assigned to 1,4-dicyanobenzene ligand-centered $^3\pi$–π^* phosphorescence which supports the activation of such radiative processes in the low temperature luminescence properties of derivatives $\mathbf{C_{Cl}}$, $\mathbf{C_{Br}}$ and $\mathbf{C_I}$. Considering these observations, it is likely that purely ligand-centered $^3\pi$–π^* phosphorescence occurs at low temperature and tends to vanish at higher temperatures due to a thermally activated interconversion between ^{3}ILCT and ^{3}MLCT states.[8,14]

Interestingly, it is worth noting that only a minor contribution of the orbital lying on the semi-bridging aqua ligand μ_2-OH_2 was observed in the electronic excitation process in the previously reported 1D-coordination polymer based on the $[Cu_2(\mu_2\text{-dppm})_2(\mu_2\text{-OH}_2]^{2+}$ dicationic unit and the 1,4-dicyanobenzene connecting ditopic ligand.[9d] Regarding the similarities in the local molecular structures of the Cu(I) dimer in this coordination polymer and the metallacycles reported herein ($[Cu_2(\mu_2\text{-dppm})_2(\mu_2\text{-OH}_2]^{2+}$ fragments *versus* $[Cu_2(\mu_2\text{-dppm})_2(\mu_2\text{-X}_2]^{+}$ moieties, X = Cl, Br, I), a similar electronic structure could explain the relatively low and unusual impact of the variation of the μ_2-bridging halide atom on the photophysical properties of metallacycles $\mathbf{C_{Cl}}$, $\mathbf{C_{Br}}$ and $\mathbf{C_I}$. Unfortunately, the computational cost of the full TD-DFT geometry optimizations of the excited states of large assemblies $\mathbf{C_{Cl}}$, $\mathbf{C_{Br}}$ and $\mathbf{C_I}$ studied here, which would allow gaining deep insights into the photophysical mechanisms, revealed to be too prohibitive to be conducted along this study. In this context, it is not straightforward to account for the origin of the high solid-state RT EQY exhibited by these metallacyclic triplet luminophores. It was previously observed that the overall multicyclic networks built in such Cu(I)-based CDS assemblies clearly induce structural constraints that significantly hamper highly detrimental non-radiative relaxation pathways and structural re-organisation in the excited states. The RT values of the k_{nr} non-radiative rate constants in this series of metallacycles reveals that non-radiative decays are quite small and more effectively suppressed in the case of lighter bridging halides. This may be related to backbones bearing shorter intermetallic distances. Indeed, on the one hand, this might be responsible for the overall lower degrees of conformational flexibilities allowed in the solid state in more compact and rigid assemblies. On the other hand, shorter intermetallic distances associated with lighter bridging halides also induce higher spin–orbit coupling constants[6b]

which impact the electronic processes, facilitating radiative de-excitation pathways. This is supported by the higher k_r radiative rate constant values obtained for the μ_2-Cl bridged derivative $\mathbf{C_{Cl}}$ (Table 3). Therefore, varying the nature of the bridging halides in this family of metallacycles leads to a dual effect, favouring the lighter halide regarding both radiative and non-radiative processes for the exaltation of the solid-state luminescence properties.

Finally, the pronounced planarity observed in the solid-state for 3,3′-bipyridine ligands **B** in $\mathbf{C_{Cl}}$, $\mathbf{C_{Br}}$ and $\mathbf{C_I}$ reveals that the coordination of these ditopic ligands on the $[Cu_2(\mu_2\text{-dppm})_2(\mu_2\text{-X})]^+$ units locks their conformation within these self-assembled metallacycles in an arrangement that promotes an efficient overlap of the π-orbitals along the quasi-planar backbones of ligands **B**. This induces the stabilization of the molecular orbitals located on these 3,3′-bipyridine ligands in $\mathbf{C_{Cl}}$, $\mathbf{C_{Br}}$ and $\mathbf{C_I}$ and supports the assumptions that ^{3}MLCT and ^{3}ILCT phosphorescence radiative relaxation processes occur in these metallacycles being based on molecular orbitals lying at least partially on connecting ligands **B**. Very likely, such conformational constrains applied on coordinated ligands **B** in derivatives $\mathbf{C_{Cl}}$, $\mathbf{C_{Br}}$ and $\mathbf{C_I}$ contribute to the differences observed between the photophysics of these metallacycles and those of the previously reported luminescent Cu(I) coordination polymer bearing 3,3′-bipyridine ligands in a twisted conformation.[10] Indeed, in the latter case, it was concluded that the recorded emission could be attributed to the delayed fluorescence from the ^{1}(M + X)LCT excited state at RT and changed to simple phosphorescence from the same triplet excited state at 77 K, suggesting radiative relaxation processes involving a larger contribution of molecular orbitals centred on the inorganic part of this derivative.[10]

Therefore, by forcing upon self-assembly processes the 3,3′-bipyridine scaffolds being almost planar (Fig. 2c), the radiative relaxation pathways in derivatives $\mathbf{C_{Cl}}$, $\mathbf{C_{Br}}$ and $\mathbf{C_I}$ are significantly altered compared to the luminescent Cu(I) coordination polymer bearing 3,3′-bipyridine ligands reported previously. This clearly demonstrates in such Cu(I)-based supramolecular assemblies the great dependence of the photophysical properties on the molecular engineering applied.

Conclusions

All in all, this study confirms the interest of synthetic approach adapting the CDS chemistry principles to conformationally flexible Cu(I) precursors. In particular, the versatility of $[Cu_2(\mu_2\text{-dppm})_2]$ bimetallic units is highlighted, revealing in the case of the use of 3-pyridyl terminated connecting ligands that it is necessary to introduce μ_2-X bridging halide ligands to lock the Cu(I) dimer fragment in a conformation that allows conducting selective CDS self-assembly processes. As a result, bimetallic node presenting potential coordination directions of *ca.* 120° are obtained. Moreover, the variety and peculiarities of the photophysical processes reported for Cu(I) CDS supramolecular assemblies are enriched with this new series of tetrametallacycles that behave as ligand centred triplet luminophores bearing a high RT EQY. These behaviours are assigned to the specific molecular organisation forced within these self-assembled structures and draw appealing perspectives for future investigations varying in particular the internal cores of the 3-pyridyl terminated connecting ligands involved in these reactions. Finally, it is worth stressing that both the gross structural parameters of these metallacycles and their photophysics in the solid-state are comparable, regardless of the nature of the bridging halide atoms. This is rather unusual and highlights on the one hand the specificities that can be associated with the use of conformationally flexible Cu(I) bimetallic precursors. On the other hand, this reveals the originality of the radiative relaxation processes that can lay in such self-assembled CDS assemblies based on the Cu(I) ion.

Author contributions

Florent Moutier: Investigation and formal analysis. Janna Schiller: Investigation and formal analysis. Guillaume Calvez: Formal analysis. Christophe Lescop: Project administration, formal analysis, and writing.

Conflicts of interest

There are no conflicts to declare.

Acknowledgements

This work was supported by the ANR (ANR PRC SMAC and ANR PRCI SUPRALUM), the CNRS, the French 'Ministère de l'Enseignement supérieur, de la Recherche et de l'Innovation' and the French 'Ministère des Affaires Etrangères'. C. L. thanks the Alexander von Humboldt Foundation for a fellowship for experienced researchers.

Notes and references

1 (*a*) J.-M. Lehn, Supramolecular chemistry: Where from? Where to?, *Chem. Soc. Rev.*, 2017, **46**, 2378; (*b*) G. Vantomme and E. W. Meijer, The Construction of Supramolecular Systems, *Science*, 2019, **363**, 1396; (*c*) J.-M. Lehn, Perspectives in Chemistry—Aspects of Adaptive Chemistry and Materials, *Angew. Chem., Int. Ed.*, 2015, **54**, 3276; (*d*) Z. Liu, S. K. M. Nalluri and J. F. Stoddart, Surveying Macrocyclic Chemistry: From Flexible Crown Ethers to Rigid Cyclophanes, *Chem. Soc. Rev.*, 2017, **46**, 2459.

2 (*a*) K. Harris, D. Fujita and M. Fujita, Giant Hollow M_nL_{2n} Spherical Complexes: Structure, Functionalisation and Applications, *Chem. Commun.*, 2013, **49**, 6703; (*b*) L. Zhang, A. J. Stephens, A. L. Nussbaumer, J.-F. Lemonnier, P. Jurček, J. Vitorica-Yrezabal and D. A. Leigh, Stereoselective Synthesis of a Composite Knot With Nine

Crossings, *Nat. Chem.*, 2018, **10**, 1083; (*c*) T. K. Ronson, Y. Wang, K. Baldridge, J. S. Siegel and J. R. Nitschke, An S_{10}-Symmetric 5-Fold Interlocked [2]Catenane, *J. Am. Chem. Soc.*, 2020, **142**, 10267; (*d*) R. Zhu, I. Regeni, J. J. Holstein, B. Dittrich, M. Simon, S. Prévost, M. Gradzielski and G. H. Clever, Catenation and Aggregation of Multi–Cavity Coordination Cages, *Angew. Chem., Int. Ed.*, 2018, **57**, 13652; (*e*) D. P. August, J. Jaramillo-Garcia, D. A. Leigh, A. Valero and I. J. Vitorica-Yrezabal, A Chiral Cyclometalated Iridium Star of David [2]Catenane, *J. Am. Chem. Soc.*, 2021, **143**, 1154; (*f*) A. W. Markwell-Heys, M. L. Schneider, J. M. L. Madridejos, G. F. Metha and W. M. Bloch, Self-Sorting of Porous $Cu_4L_2L'_2$ Metal-Organic Cages Composed of Isomerisable Ligands, *Chem. Commun.*, 2021, **57**, 2915; (*g*) X. Hu, S. Feng, J. Du, L. Shao, J. Lang, C. Zhang, S. P. Kelley, J. Lin, S. J. Dalgarno, D. A. Atwood and J. L. Atwood, Controlled Hierarchical Self-Assembly of Networked Coordination Nanocapsules via the Use of Molecular Chaperones, *Chem. Sci.*, 2020, **11**, 12547; (*h*) J. Shi, Y. Li, X. Jiang, H. Yu, J. Li, H. Zhang, D. J. Trainer, S. W. Hla, H. Wang, M. Wang and X. Li, Self-Assembly of Metallo-Supramolecules with Dissymmetrical Ligands and Characterization by Scanning Tunneling Microscopy, *J. Am. Chem. Soc.*, 2021, **143**, 1224; (*i*) D. Liu, K. Li, M. Chen, T. Zhang, Z. Li, J.-F. Yin, L. He, J. Wang, P. Yin, Y.-T. Chan and P. Wang, Russian-Doll-Like Molecular Cubes, *J. Am. Chem. Soc.*, 2021, **143**, 2537; (*j*) M. R. Crawley, D. Zhang, A. N. Oldacre, C. M. Beavers, A. E. Friedman and T. R. Cook, Tuning the Reactivity of Cofacial Porphyrin Prisms for Oxygen Reduction Using Modular Building Blocks, *J. Am. Chem. Soc.*, 2021, **143**(2), 1098; (*k*) B. Li, W. Zhang, S. Lu, B. Zheng, D. Zhang, A. Li, X. Li, X.-J. Yang and B. Wu, Multiple Transformations among Anion-based $A_{2n}L_{3n}$ Assemblies: Bicapped Trigonal Antiprism A_8L_{12}, Tetrahedron A_4L_6, and Triple Helicate A_2L_3 (A=Anion), *J. Am. Chem. Soc.*, 2020, **142**, 21160; (*l*) D. Yang, J. L. Greenfield, T. K. Ronson, L. K. S. von Krbek, L. Yu and J. R. Nitschke, La^{III} and Zn^{II} Cooperatively Template a Metal–Organic Capsule, *J. Am. Chem. Soc.*, 2020, **142**, 19856; (*m*) S. Fang, M. H.-Y. Chan and V. W.-W. Yam, Dinuclear Anthracene Containing Alkynylplatinum(II) Terpyridine Complexes with Photo-modulated Self-Assembly Behaviors, *Mater. Chem. Front.*, 2021, **5**, 2409; (*n*) Q. Tu, G.-F. Huo, X.-L. Zhao, H. Sun, X. Shi and H.-B. Yang, Facile Construction of Well-Defined Radical Metallacycles through Coordination-Driven Self-Assembly, *Mater. Chem. Front.*, 2021, **5**, 1863; (*o*) Z.-T. Shi, Y.-X. Hu, Z. Hu, Q. Zhang, S.-Y. Chen, M. Chen, J.-J. Yu;, G.-Q. Yin, H. Sun, L. Xu, X. Li, B. L. Feringa, H.-B. Yang, H. Tian and D.-H. Qu, Visible-Light-Driven Rotation of Molecular Motors in Discrete Supramolecular Metallacycles, *J. Am. Chem. Soc.*, 2021, **143**, 442; (*p*) C. Mu, Z. Zhang, Y. Hou, H. Liu, L. Ma, X. Li, S. Ling, G. He and M. Zhang, Tetraphenylethylene–Based Multicomponent Emissive Metallacages as Solid–State Fluorescent Materials, *Angew. Chem., Int. Ed.*, 2021, **22**, 12293; (*q*) Y. Li, S. S. Rajasree, G. Y. Lee, J. Yu, J.-H. Tang, R. Ni, G. Li, K. N. Houk, P. Deria and P. J. Stang, Anthracene-Triphenylamine-Based Platinum(II) Metallacages as Synthetic Light-Harvesting Assembly, *J. Am. Chem. Soc.*, 2021, **143**, 2908; (*r*) S. Sudan, R.-J. Li, S. M. Jansze, A. Platzek, R. Rudolf, G. H. Clever, F. Fadaei-Tirani, R. Scopelliti and K. Severin, Identification of a Heteroleptic $Pd_6L_6L'_6$ Coordination Cage by Screening of a Virtual Combinatorial Library, *J. Am. Chem. Soc.*, 2021, **143**, 1773; (*s*) L.-X. Cai, D.-N. Yan, P.-M. Cheng, J.-J. Xuan, S.-C. Li, L.-P. Zhou, C.-B. Tian and Q.-F. Sun, Controlled Self-Assembly and Multistimuli-Responsive Interconversions of Three Conjoined Twin-Cages, *J. Am. Chem. Soc.*, 2021, **143**, 2016; (*t*) W.-L. Jiang, Z. Peng, B. Huang, X.-L. Zhao, D. Sun, X. Shi and H.-B. Yang, TEMPO Radical-Functionalized Supramolecular Coordination Complexes with Controllable Spin–Spin Interactions, *J. Am. Chem. Soc.*, 2021, **143**, 433; (*u*) R.-J. Li, J. Tessarolo, H. Lee and G. H. Clever, Multi-stimuli Control over Assembly and Guest Binding in Metallo-suparmolecular Hosts Based on Dithienylethene Photoswitches, *J. Am. Chem. Soc.*, 2021, **143**, 3865; (*v*) I. Regeni, B. Chen, M. Frank, A. Baksi, J. J. Holstein and G. H. Clever, Coal-Tar Dye-Based Coordination Cages and Helicates, *Angew. Chem.*, 2021, **60**, 5673.

3 (*a*) S. R. Seidel and P. J. Stang, High-Symmetry Coordination Cages via Self-Assembly, *Acc. Chem. Res.*, 2002, **35**, 972; (*b*) M. Fujita, M. Tominaga, A. Hori and B. Therrien, Coordination Assemblies from a Pd(II)-cornered square complex, *Acc. Chem. Res.*, 2005, **38**, 369; (*c*) T. R. Cook and P. J. Stang, Recent Developments in the Preparation and Chemistry of Metallacycles and Metallacages via Coordination, *Chem. Rev.*, 2015, **115**, 7001; (*d*) S. Saha, I. Regeni and G. H. Clever, Structure relationships between bis-monodentate ligands and coordination driven self-assemblies, *Coord. Chem. Rev.*, 2018, **374**, 1; (*e*) L. Xu, Y.-X. Wang, L.-J. Chen and H.-B. Yang, Construction of Multiferrocenyl Metallacycles and Metallacages via Coordination-Driven Self-Assembly: From Structure to Functions, *Chem. Soc. Rev.*, 2015, **44**, 2148; (*f*) N. C. Gianneschi, M. S. Masar III and C. A. Mirkin, Development of a Coordination Chemistry-Based Approach for Functional Supramolecular Structures, *Acc. Chem. Res.*, 2005, **38**, 825; (*g*) M. Scheer, The Coordination Chemistry of Group 15 Element Ligand Complexes—a Developing Area, *Dalton Trans.*, 2008, 4372.

4 (*a*) D. Bardhan and D. K. Chand, Palladium(II)-Based Self-Assembled Heteroleptic Coordination Architectures: A Growing Family, *Chem. – Eur. J.*, 2019, **25**, 12241; (*b*) S. Pullen and G. H. Clever, Mixed-Ligand Metal-Organic Frameworks and Heteroleptic Coordination Cages as Multifunctional Scaffolds – A Comparison, *Acc. Chem. Res.*, 2018, **51**, 3052; (*c*) Y. Sun, C. Chen, J. Lin and P. J. Stang, Recent Developments in the Construction and Applications of Platinum-Based Metallacycles and Metallacages via Coordination, *Chem. Soc. Rev.*, 2020, **49**, 3889.

5 (*a*) N. Sinha and F. E. Hahn, Metallosupramolecular Architectures Obtained from Poly-N-Heterocyclic Carbene

Ligands, *Acc. Chem. Res.*, 2017, **50**, 2167; (*b*) J. Dong, Y. Pan, H. Wang, K. Yang, L. Liu, Z. Qiao, Y. Di, Y. Shing, B. Peh, J. Zhang, L. Shi, H. Liang, Y. Han, X. Li, J. Jiang, B. Liu and D. Zhao, Self–Assembly of Highly Stable Zirconium(IV) Coordination Cages with Aggregation Induced Emission Molecular Rotors for Live–Cell Imaging, *Angew. Chem.*, 2020, **59**, 10151; (*c*) J. Schiller, E. Peresypkina, A. V. Virovets and M. Scheer, Metal-Deficient Supramolecule Based on a Fivefold-Symmetric Building Block, *Angew. Chem.*, 2020, **59**, 13647; (*d*) D. Zhang, T. K. Ronson and J. R. Nitschke, Functional Capsules via Subcomponent Self-Assembly, *Acc. Chem. Res.*, 2018, **51**, 2423; (*e*) S. M. Jansze and K. Severin, Clathrochelate Metalloligands in Supramolecular Chemistry and Materials Science, *Acc. Chem. Res.*, 2018, **51**, 2139; (*f*) C. Lescop, Coordination-Driven Syntheses of Compact Supramolecular Metallacycles toward Extended Metallo-Organic Stacked Supramolecular Assemblies, *Acc. Chem. Res.*, 2017, **50**, 885.

6 (*a*) C. Lescop, Coordination-Driven Supramolecular Synthesis Based on Bimetallic Cu(I) Precursors : Adaptive Behavior and Luminescence, *Chem. Rec.*, 2020, **21**, 544; (*b*) M. El Sayed Moussa, S. Evariste, H.-L. Wong, L. Le Bras, C. Roiland, L. Le Polles, B. Le Guennic, K. Costuas, V. W.-W. Yam and C. Lescop, A solid state highly emissive Cu (I) metallacycle: promotion of cuprophilic interactions at the excited states, *Chem. Commun.*, 2016, **52**, 11370; (*c*) S. Evariste, A. M. Khalil, M. El Sayed Moussa, A. K.-W. Chan, E. Y.-H. Hong, H.-L. Wong, B. Le Guennic, G. Calvez, K. Costuas, V. W.-W. Yam and C. Lescop, Adaptive Coordination-Driven Supramolecular Syntheses toward New Polymetallic Cu(I) Luminescent Assemblies, *J. Am. Chem. Soc.*, 2018, **140**, 12521; (*d*) M. El Sayed Moussa, A. M. Khalil, S. Evariste, H.-L. Wong, V. Delmas, B. Le Guennic, G. Calvez, K. Costuas, V. W.-W. Yam and C. Lescop, Intramolecular Rearrangements Guided by Adaptive Coordination-Driven Reactions toward Highly Luminescent Polynuclear Cu(I) Assemblies, *Inorg. Chem. Front.*, 2020, **7**, 1334; (*e*) S. Evariste, M. El Sayed Moussa, H.-L. Wong, G. Calvez, V. W.-W. Yam and C. Lescop, Straightforward Preparation of a Solid-state Luminescent Cu_{11} Polymetallic Assembly via Adaptive Coordination-driven Supramolecular Chemistry, *Z. Anorg. Allg. Chem.*, 2020, **646**, 754.

7 (*a*) H. Yersin, *Highly Efficient OLEDS: Materials Based on Thermally Activated Delayed Fluorescence*, Wiley–VCH Verlag GmbH & Co, 2019; (*b*) V. W.-W. Yam, V. K.-M. Au and S. Y.-L. Leung, Light-Emitting Self-Assembled Materials Based on d^8 and d^{10} Transition Metal Complexes, *Chem. Rev.*, 2015, **115**, 7589; (*c*) R. Czerwieniec, M. J. Leitl, H. H. H. Homeier and H. Yersin, Thermally Cu(I) Complexes – Thermally activated delayed fluorescecnce. Photophysical approach and material design, *Coord. Chem. Rev.*, 2016, **325**, 2; (*d*) A. Kobayashi and M. Kato, Stimuli-responsive Luminescent Copper(I) Complexes for Intelligent Emissive Devices, *Chem. Lett.*, 2017, **46**, 154; (*e*) Q. Benito, X. Le Goff, S. Maron, A. Fargues, A. Garcia, C. Martineau, F. Taulelle, S. Kahlal, T. Gacoin, J.-P. Boilot and S. Perruchas, Polymorphic Copper Iodide Clusters: Insights into the Mechanochromic Luminescence Properties, *J. Am. Chem. Soc.*, 2014, **136**, 11311; (*f*) B. Huitorel, H. El Moll, R. Utrera-Melero, M. Cordier, A. Fargues, A. Garcia, F. Massuyeau, C. Martineau-Corcos, F. Fayon, A. Rakhmatullin, S. Kahlal, J.-Y. Saillard, T. Gacoin and S. Perruchas, Evaluation of Ligands Effect on the Photophysical Properties of Copper Iodide Clusters, *Inorg. Chem.*, 2018, **57**, 4328; (*g*) J. Nitsch, F. Lacemon, A. Lorbach, A. Eichhorn, F. Cisnetti and A. Steffen, Cuprophilic Interactions in Highly Luminescent Dicopper (I)-NHC-Picolyl Complexes – Fast Phosphorescence or TADF, *Chem. Commun.*, 2016, **52**, 2932; (*h*) B. Hupp, J. Nitsch, T. Schmitt, R. Bertermann, K. Edkins, F. Hirsch, I. Fischer, M. Auth, A. Sperlich and A. Steffen, Stimulus-Triggered Formation of an Anion-Cation Exciplex in Copper (I) Complexes as a Mechanism for Mechanochromic Phosphorescence, *Angew. Chem., Int. Ed.*, 2018, **57**, 13671; (*i*) B. Hupp, C. Schiller, C. Lenczyk, M. Stanoppi, K. Edkins, A. Lorbach and A. Steffen, Synthesis, Structures, and Photophysical Properties of a Series of Rare Near-IR Emitting Copper(I) Complexes, *Inorg. Chem.*, 2017, **56**, 8996; (*j*) T. Hasegawa, A. Kobayashi, H. Ohara, M. Yoshida and M. Kato, Emission Tunin of Luminescent Copper(I) Complexes by Vapor-Induced Ligand Exchange Reactions, *Inorg. Chem.*, 2017, **56**, 4928; (*k*) C. Zheng, N. Wang, T. Peng and S. Wang, Copper(I) Complexes Bearing 1,2-Phenyl-Bridged P^N, P^N^P, and N^P^N Chelate Ligands: Structures and Phosphorescence, *Inorg. Chem.*, 2017, **56**, 1616; (*l*) A. Kobayashi, M. Fujii, Y. Shigeta, M. Yoshida and M. Kato, Quantitative Solvent-Free Thermal Synthesis of Luminescent Cu(I) Coordination Polymers, *Inorg. Chem.*, 2019, **58**, 4456; (*m*) A. Kobayashi, Y. Yoshida, M. Yoshida and M. Kato, Mechanochromic Switching between Delayed Fluorescence and Phosphorescence of Luminescent Coordination Polymers Composed of Dinuclear Copper(I) Iodide Rhombic Cores, *Chem. – Eur. J.*, 2018, **24**, 14750; (*n*) P. Liang, A. Kobayashi, W. M. C. Sameera, M. Yoshida and M. Kato, Solvent-Free Thermal Synthesis of Luminescent Dinuclear Cu(I) Complexes with Triarylphosphines, *Inorg. Chem.*, 2018, **57**, 5929; (*o*) A. V. Artem'ev, M. R. Ryzhikov, I. V. Taidakov, M. I. Rakhmanova, E. A. Varaksina, I. Y. Bagryanskaya, S. F. Malysheva and N. A. Belogorlova, Bright Green-to-Yellow Emitting Cu(i) Complexes based on Bis(2-pyridyl) phosphine Oxides: Synthesis, Structure and Effective Thermally Activated-Delayed Fluorescence, *Dalton Trans.*, 2018, **47**, 2701; (*p*) A. V. Artem'ev, E. A. Pritchina, M. I. Rakhmanova, N. P. Gritsan, I. Y. Bagryanskaya, S. F. Malysheva and N. A. Belogorlova, Alkyl-Dependent Self-Assembly of the First Red-Emitting Zwitterionic $\{Cu_4I_6\}$ Clusters from $\{alkyl\text{-}P(2\text{-}Py)_3\}^+$ Salts and CuI: When Size Matters, *Dalton Trans.*, 2019, **48**, 2328; (*q*) G. Chakkaradhari, T. Eskelinen, C. Degbe, A. Belyaev, A. S. Melnikov, E. V. Grachova, S. P. Tunik, P. Hirva and

I. O. Koshevoy, Oligophosphine-thiocyanate Copper(I) and Silver(I) Complexes and Their Borane Derivatives Showing Delayed Fluorescence, *Inorg. Chem.*, 2019, **58**(6), 3646–3660; (*r*) G. Chakkaradhari, Y.-T. Chen, A. J. Karttunen, M. T. Dau, J. Jänis, S. P. Tunik, P.-T. Chou, M.-L. Ho and I. O. Koshevoy, Luminescent Triphosphine Cyanide d^{10} Metal Complexes, *Inorg. Chem.*, 2016, **55**(5), 2174–2184; (*s*) R. Hamze, J. L. Peltier, D. Sylvinson, M. Jung, J. Cardenas, R. Haiges, M. Soleilhavoup, R. Jazzar, P. I. Djurovich, G. Bertrand and M. E. Thompson, Eliminating nonradiative decay in Cu(I) emitters: >99% quantum efficiency and microsecond lifetime, *Science*, 2019, **363**, 601; (*t*) S. Shi, M. Chul Jung, C. Coburn, A. Tadle, M. R. D. Sylvinson, P. I. Djurovich, S. R. Forrest and M. E. Thompson, Highly Efficient Photo- and Electroluminescence from Two-Coordinate Cu(I) Complexes Featuring Nonconventional N-Heterocyclic Carbenes, *J. Am. Chem. Soc.*, 2019, **141**, 3576; (*u*) S. Evariste, C. Xu, G. Calvez and C. Lescop, Straightforward Coordination-Driven Supramolecular Chemistry Preparation of a Discrete Solid-State Luminescent Cu_4 Polymetallic Compact Assembly Based on Conformationally Flexible Building Blocks, *Inorg. Chim. Acta*, 2021, **516**, 120115; (*v*) M. Gernert, L. Balles-Wolf, F. Kerner, U. Müller, A. Schmiedel, M. Holzapfel, C. M. Marian, J. Pflaum, C. Lambert and A. Steffen, Cyclic (Amino)(aryl)carbenes Enter the Field of Chromophore Ligands: Expanded π System Leads to Unusually Deep Red Emitting Cu^{I} Compounds, *J. Am. Chem. Soc.*, 2020, **142**, 8897; (*w*) M. Olaru, E. Rychagova, S. Ketkov, Y. Shynkarenko, S. Yakunin, M. V. Kovalenko, A. Yablonskiy, B. Andreev, F. Kleemiss, J. Beckmann and M. Vogt, A Small Organo-Copper Cluster as Thermally Robust Highly Photo- and Electroluminescent Material, *J. Am. Chem. Soc.*, 2020, **142**, 373; (*x*) A. V. Artem'ev, M. P. Davydova, A. S. Berezin, M. R. Ryzhikov and D. G. Samsonenko, Dicopper(I) Paddle-Wheel Complexes with Thermally Activated Delayed Fluorescence Adjusted by Ancillary Ligands, *Inorg. Chem.*, 2020, **59**, 10699; (*y*) J. Troyano, F. Zamora and S. Delgado, Copper(I)-Iodide Cluster Structures as Functional and Processable Platform Materials, *Chem. Soc. Rev.*, 2021, **50**, 4606; (*z*) A. V. Artem'ev, A. Y. Baranov, E. A. Pritchina, A. S. Berezin, N. P. Gritsan, D. G. Samsonenko, V. P. Fedin and N. A. Belogorlova, *Angew. Chem., Int. Ed.*, 2021, **60**, 12577.

8 (*a*) Y. Zhang, M. Schulz, M. Wächtler, M. Karnahl and B. Dietzek, Heteroleptic diamine-diphosphine Cu(I) Complexes as an Alternative Towards Noble-Metal Based Photosensitizers: Design Strategies, Photophysical Properties and Perspective Applications, *Coord. Chem. Rev.*, 2018, **356**, 127.

9 (*a*) B. Nohra, Y. Yao, C. Lescop and R. Réau, Coordination Polymers with p-Stacked Metalloparacyclophane Motifs: F-Shaped Mixed-Coordination Dinuclear Connectors, *Angew. Chem., Int. Ed.*, 2007, **46**, 8242; (*b*) F. Moutier, A. M. Khalil, S. Baudron and C. Lescop, Gleaned Snapshots on the Road to Coordination Polymers: Heterometallic Architectures Based on Cu(I) Metallaclips and 2,2′-bis-dipyrrin Metalloligands, *Chem. Commun.*, 2020, **56**, 10501; (*c*) M. El Sayed Moussa, S. Evariste, B. Krämer, R. Réau, M. Scheer and C. Lescop, Can Coordination-Driven Supramolecular Self-Assembly Reactions Be Conducted from Fully Aliphatic Linkers?, *Angew. Chem., Int. Ed.*, 2018, **57**, 795; (*d*) S. Evariste, A. M. Khalil, S. Kerneis, C. Xu, G. Calvez, K. Costuas and C. Lescop, Luminescent Vapochromic Single Crystal to Single Crystal Transition in One-Dimensional Coordination Polymer Featuring the First Cu(I) Dimer Bridged by an Aqua Ligand, *Inorg. Chem. Front.*, 2020, **7**, 3402.

10 (*a*) W. Liu, Y. Fang, G. Z. Wei, S. J. Teat, K. Xiong, Z. Hu, W. P. Lustig and J. Li, A Family of Highly Efficient CuI-Based Lighting Phosphors Prepared by a Systematic, Bottom-up Synthetic Approach, *J. Am. Chem. Soc.*, 2015, **137**, 9400; (*b*) A. Kobayashi, M. Fujii, Y. Shigeta, M. Yoshida and M. Kato, Quantitative Solvent-Free Thermal Synthesis of Luminescent Cu(I) Coordinaton Polymers, *Inorg. Chem.*, 2019, **58**, 4456.

11 (*a*) S. Naik, J. T. Mague and M. S. Balakrishna, Short-Bite PNP Ligand-Supported Rare Tetranuclear [Cu4I4] Clusters: Structural and Photoluminescence Studies, *Inorg. Chem.*, 2014, **53**, 3864; (*b*) N. V. Satyachand Harisomayajula, S. Makovetskyi and Y.-C. Tsai, Cuprophilic interactions in and between Molecular Entities, *Chem. – Eur. J.*, 2019, **25**, 8936.

12 (*a*) E. Rodriguez-Sanz, C. Lescop and R. Réau, A Cu(I) cluster bearing a bridging phosphane ligand, *C. R. Chim.*, 2010, **13**, 980; (*b*) C. W. Liu, B.-J. Liaw, L.-S. Liou and J.-C. Wang, A 2D Honeycomb-Shaped Network Based on a Starburst Cluster: $[Ag_4(\mu_3\text{-}Cl)(PPh_2(CH_2)_2PPh_2)_{1.5}\{S_2P(OR)_2\}_3]$ (R=Et, Pr^i), *Chem. Commun.*, 2005, 1983; (*c*) B.-J. Liaw, T. S. Lobana, Y.-W. Lin, J.-C. Wang and C. W. Liu, Versatility of Dithiophosphates in the Syntheses of Copper(I) Complexes with Bis(diphenylphosphino) alkanes: Abstraction of Chloride from Dichloromethane, *Inorg. Chem.*, 2005, **44**, 9921; (*d*) C. E. Anson, L. Ponikiewski and A. Rothenberger, Halide Abstraction from Organic Solvents in Reactions of a Copper(I) Alkoxide: Synthesis and Crystal Structures of $[Cu_5(dppm)(dppm^{-})_2(O^tBu)Cl_2]$ and $[Cu_3(dppm)_3Br_2][CuBr_2]$, *Z. Anorg. Allg. Chem.*, 2006, **632**, 2402; (*e*) K. J. Doyle, H. Tran, M. Baldoni-Olivencia, M. Karabulut and P. E. Hoggard, Photocatalytic degradation of Dichloromethane by Chlorocuprate(II) Ions, *Inorg. Chem.*, 2008, **47**, 7029.

13 S. Dey, D. Buzsáki, C. Bruhn, Z. Kelemen and R. Pietschnig, Bulky 1,1′-bisphosphanoferrocenes and their coordination behaviour towards Cu(I), *Dalton Trans.*, 2020, **49**, 6668.

14 (*a*) D. J. Casadonte Jr. and D. R. McMillin, Hindered Internal Conversion in Rigid Media. Thermally Non-Equilibrated 3IL and 3CT Emissions from $[Cu(5\text{-}X\text{-}phen)(PPh_3)_2]^+$ and $[Cu(4,7\text{-}X2\text{-}phen)(PPh_3)_2]^+$ Systems in a Glass at 77 K, *J. Am. Chem. Soc.*, 1987, **109**, 331; (*b*) W. L. Parker and G. A. Crosby, Assignment of the Charge-Transfer Excited States of bis(N-heterocyclic) Complexes of Copper (I), *J. Phys. Chem.*, 1989, **93**, 5692.

